20

Sailcraft Trajectories

We are nearing the end of this introductory book on solar sailing. We saved one of the most intriguing topics—trajectory design—in the end. Although, in Chap. 19, we reported some key equations for showing the physical meaning and usefulness of the lightness vector formalism, nevertheless it is beyond the scope of this book to delve *deeply* into mathematics and the related physical aspects. Therefore, after a very short presentation of the sailcraft motion equations, we discuss the class of trajectories (and missions) via several technical plots. Some trajectories have been designed in past decades, some were investigated in the first years of this century, and some have been calculated specifically for this book by means of modern (and very complex) computer codes. In this chapter, we deal with:

1. sailcraft motion equations in their simple form by using no additional mathematics;
2. generalized Keplerian orbits that only sailcraft can draw;
3. interplanetary transfer by solar sailing;
4. some of the new striking features solar-sail propulsion offers, such as the possibility of designing orbits that differ from the Keplerian ones significantly, allowing a mission designer to move beyond the limits of conventional spacecraft;
5. the behavior of a sailcraft under the gravitational influence of more than one celestial body;
6. the so-called artificial equilibrium points;
7. the high non-linear feature of very low sail-loading sailcraft.

MOTION EQUATIONS

Formally, the classical motion equations of spacecraft are not complicated. But in addition to the difficulty, common to any scientific discipline, of modeling the real world, in Astrodynamics there is the need to optimize trajectories with respect to some performance criterion related to the mission goals. Furthermore, one has to solve equations numerically,

G. Vulpetti et al., *Solar Sails*, Springer Praxis Books,
DOI 10.1007/978-1-4939-0941-4_20

which may seem a trivial task, at first glance, in the modern era of high-level software and computers. However, the opposite is true. Judicious choices of calculation units, reference frames, switching from one frame to another (when applicable), numeric integrators, optimization methods, and computing additional information (useful for understanding the many aspects of the problems) are all delicate procedures for achieving reliable results upon which a mission may be designed. There is an incredible amount of high-level literature on these topics. We cite a few studies in the course of this chapter relatively to the sailcraft trajectories we are discussing.

In the inertial reference frame (IF) where one wants to describe the sailcraft motion, let **r** denote the position vector of the sailcraft, namely, the vector from the origin of IF to the sailcraft's barycenter. Often, the IF origin coincides with the center of mass of a celestial body in the solar system (the Sun or any planet), which is taken as the central body. Let $GM \equiv \mu$ indicate the gravitational mass of such a *central* body. Then, the equation of motion can be written as follows:

$$\frac{d^2\mathbf{r}}{dt^2} = -\mu_* \mathbf{r} / r^3 + P + \left(\mu_\odot / R^2\right) \Phi \mathbf{L} \tag{20.1}$$

where the subscript * stands for the Sun ($\odot$), Earth ($\otimes$), or any other planet. Let us explain the meaning of this vector equation. Like any classical motion equation, the left-hand side (l.h.s.) represents the vector acceleration (a pure kinematical quantity). The right-hand side (r.h.s.) includes all dynamical contributions, namely, the forces per unit mass that act upon the space vehicle. The first term on the (r.h.s.) represents the gravitational vector acceleration due to the central body; ***P*** denotes the overall perturbation acceleration stemming from conservative or non-conservative fields (but propulsion), whereas the third term is the solar-sail thrust acceleration due to the sunlight's solar pressure, as described in other chapters of this book. R is the distance from the sailcraft to the Sun, **L** is the sailcraft lightness vector defined in Eq. (19.3) in Chap. 19. Finally, Φ is the rotation matrix from SOF (the reference frame defined in Chap. 19) to HIF. Such a matrix transforms the **L**'s components in SOF to those in the current inertial reference frame. The degradation of the sail's reflectance (Chap. 21) should not be included in an equation of this type. However, as discussed in Chap. 19, one can include varying-with-sunlight incidence reflection and absorption in this equation.

Therefore, for our purposes, the above equation of motion can be considered general. Of course, we have to specify either initial conditions (the initial value problem) or mixed information regarding the initial and final state (the two-boundary problem) of the sailcraft in order to integrate such second-order differential equation *numerically.* However, that is not enough. Like any differential equation containing free parameters, or *controls,* Eq. (20.1) needs a time profile of such controls in order to be solved completely. How may we specify such control behaviors? Normally, in designing a trajectory (or a set of trajectories) for a space mission with given payload goals, one has to identify *three* important classes of linear/non-linear constraints and some objective function: (1) state equality/inequality constraints, (2) control equality/inequality constraints, and (3) mixed state and control constraints. Classes 1 and 2 in particular are characteristic of the set of admissible trajectories, whereas class 3 is the direct consequence of the optimization problem at hand.

Designing space missions based on rocket propulsion has a strong feature: minimizing the propellant during the transfer-to-target phase and during the operational mission (orbit and attitude control). In contrast, sailcraft-based space missions will be characterized—among the many features we have highlighted in the previous chapters—by two noteworthy aspects: (1) strongly minimizing the transfer time (e.g. avoiding multiple planetary flybys), and (2) achieving controlled operational configurations without using propellant of any type. These aspects often are impossible to accomplish via rocket propulsion. Optimization criterion (1) is important not only for cutting mission costs and a number of equally significant nontechnical issues, but also for reducing the degradation of the reflective layer of the sail, another significant objective indeed.

Equation (20.1) may contain the contribution to non-Keplerian acceleration coming from the pressure of the light backscattered or emitted by a planet or a natural satellite (where applicable). Because *planetary-radiation* thrust acceleration is always much weaker than *solar*-radiation thrust acceleration (due to planet temperature that is very low compared to the solar one, the planetary albedo, considerable absorbing and scattering planet atmosphere, etc.), nobody thinks of using the planet's radiation for controlling the trajectory of a sailcraft. Instead, this acceleration—even if modeled in computer codes (at least in the most sophisticated ones)—may be dealt with as a perturbation to sailcraft spiraling about a planet. Therefore, it can be considered as included in the term $\boldsymbol{P}$ of Eq. (20.1), which mainly contains gravitational perturbations, caused by celestial bodies other than the central body, and its aspherical shape.

GENERAL KEPLERIAN ORBITS

The best way to see the effects of solar-radiation thrust is to analyze a number of very special trajectory classes by first removing the perturbation term from Eq. (20.1) and considering heliocentric sail trajectories. In addition, let us suppose that the sail *direction* is always parallel to the local sunlight (i.e. its surface is perpendicular to sunlight direction). From the general equation, one gets

$$\frac{d^2\mathbf{R}}{dt^2} = -\left(1-l_x\right)\frac{\mu_\odot}{R^3}\mathbf{R} \tag{20.2}$$

where l_x is the radial lightness number defined in Chap. 16. This equation is the differential equation governing all possible *general* Keplerian orbits. Conceptually, they are very simple: the sailcraft senses the Sun with an *effective* gravitational mass $\tilde{\mu}_\odot = \left(1-l_x\right)\mu_\odot$. Depending on the technology that we will utilize progressively in future solar sailing, $\tilde{\alpha}_\odot$ may become negative too; that is, the sum of the solar gravity and the solar-radiation effect can be *repulsive* on the sailcraft. In the special case that the radial number is identically one (that is, $l = l_x = 1$ and $\sigma = \tau\sigma_c$ from Note 3 in Chap. 19), the sailcraft can move uniformly on a rectilinear trajectory, with speed and direction depending on the initial conditions, in the solar system. (Perturbations alter this ideal state, of course.) This property lends itself to intriguing interplanetary transfers. Such an advanced-sail and spacecraft technology would allow sailcraft to spiral fast (1 month at most) about Earth and to escape

the Earth–Moon system with a residual speed of 1–2 km/s. Thus, the heliocentric speed may amount to 6.5–6.7 AU/year. The velocity direction is approximately perpendicular to the position vector of the Earth, and in Earth's heliocentric orbit plane, at the exiting time. (More generally, such property holds for any sailcraft with $l_x = 1$, and leaving any planet.) After a rectilinear arc, the sail would be tilted so as to progressively match the heliocentric vector velocity of the target planet (e.g., Mars). If we include the spiral time about Mars, the whole Earth-to-Mars transfer should last half the time of the current flights to the red planet. However, the main advantage would be that most of the heliocentric trajectory would be orthogonal to the departure-planet vector position, as stated above, with the immediate consequence of relaxing the launch window considerably; in other words, going to Mars would not need to wait for favorable Earth–Mars relative positions. A similar thing would apply for the return trip. Thus, a reusable sailcraft may accomplish round-trips to Mars twice as fast and with low dependence on the planetary positions! Since the sail technology for such flights is somewhat advanced with respect to that available today, missions like this one have not yet been studied carefully. (At the time of this writing, preliminary research was in progress in Italy about the possibility of using special carbon nanotube membranes for future applications to solar sailing, though we are not yet able to estimate how far in the future all this may take place.)

Other interesting novel solutions happen if $0 < l_x < 1$. They are the subject of the rest of this section. Let consider a heliocentric circular orbit obeying Eq. (20.2). What is the period of such an orbit? Figure 20.1 shows period values as a function of the orbit radius and the radial number.

Note 1: The circular-orbit solutions to Eq. (20.2) correspond to orbits with the sail *already* deployed. If the spacecraft initially orbits about the Sun circularly with the sail unfolded and subsequently opens its sail radially, then the orbit transforms into an elliptic, parabolic or hyperbolic, depending on the radial number. The sailcraft pre-deployment speed has to be lower than the usual circular value $\sqrt{\infty_\odot / R}$ for getting a sail-open circular orbit. For instance, the deployment maneuver can happen at the aphelion of a pure Keplerian ellipse.

In Fig. 20.1, note the curve representing the 1-year period orbits. In particular, one can envisage a sailcraft on the same plane of Earth orbit and 0.3 AU sunward and always on the same Sun–Earth line. (This is analogous to what happens close to the Sun–Earth system L1 point; however, L1 is 1.5 million km or 0.01 AU far from Earth). This sail mission concept requires $l_x = 0.657$, namely, a technology considerably more advanced than the current one. Such mission could be not only scientific but also utilitarian. Among other things, as anticipated in Chap. 9, the space-storm warning time would range from 16 to 31 h instead of the current 70–90 min from L1 (including the lower-speed path of the solar wind in Earth's magnetopause).

Implicit in Note 1 is that Fig. 20.1 holds for any elliptic orbit of a sailcraft about the Sun. We suggest college students starting from Eq. (20.2) and carry out some general formulas (e.g., energy, angular momentum, eccentricity, semimajor axis, etc.) useful to evaluate the performance of a sailcraft with respect to a classical spacecraft capable of rocket maneuver. As a point of fact, the sail deployment may be viewed as an impulsive maneuver with no propellant consumption. For a spacecraft orbiting about the Sun on any circular path, deploying a sail—completely sunward and with lightness number equal to

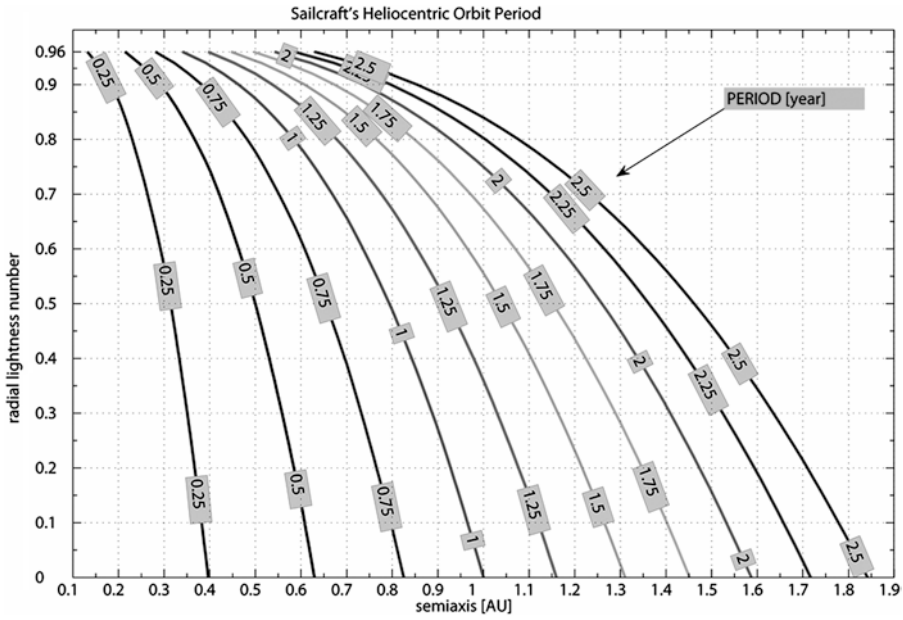

20.1 Contours of the period (year) of a general Keplerian orbit as a function of the semimajor axis (AU) and the radial lightness number

½—inserts the vehicle into a parabolic orbit. The open interval (1/2, 1) entails a hyperbolic orbit with some excess velocity.

With the concepts established so far, we are able to apply a sail mission concept studied years ago by author Matloff. The following is an ideal mission from some viewpoints; nevertheless, it will be useful for defining the concepts of fast and very-fast solar sailing modes, which we will deal with later in this chapter. Suppose that a spacecraft has two propulsion systems: (1) an impulsive rocket engine, and (2) a photon solar sail. Some launcher delivers the vehicle to about 2.7 million km from Earth where the solar field dominates. Let us assume that the rocket is capable of releasing a velocity impulse equal to $\left(\sqrt{2}-1\right)/\sqrt{R_0}$ (or 12.3 km/s at $R_0=1$ AU, very large indeed). Were such impulse applied parallel to Earth's orbital velocity at that point ($\mathbf{V_E}$), the spacecraft would escape the solar system on a parabola. One knows that in such a case the speed at infinity is $V_\infty=0$. However, let us apply the same impulse antiparallel to $\mathbf{V_E}$. The ensuing orbit is elliptic sunward and the vehicle can achieve the perihelion $R_P=½\left(\sqrt{2}-1\right)R_0$ (or 0.207 AU) after about 85.5 days (during which the rocket system has been jettisoned). Here, the sail comes into play. Let us suppose (1) we deploy the sail in a very brief time interval and radially, having designed the sailcraft with $l_x=1$, (2) to keep the sail radial from that moment on. The scenario, which we may call the *CRS* (combined rocket-sail) reference flight, is depicted in Fig. 20.2. The ensuing motion is rectilinear and uniform with a speed equal to twice the parabolic speed at R_0, namely, 84.24 km/s or about 17.77 AU/year. This value is five times the speed of Voyager 1, the fastest spacecraft launched hitherto.

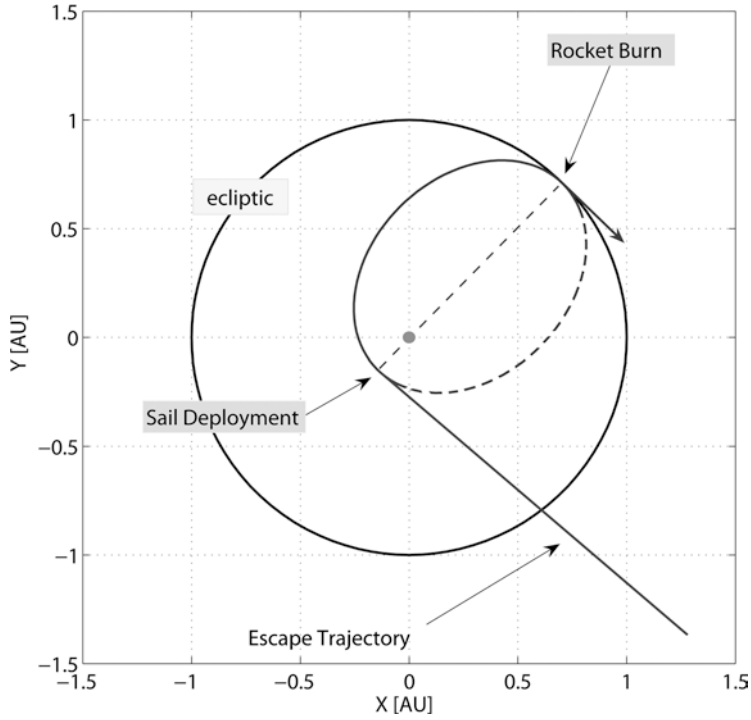

20.2 Ideal *two-propulsion* reference mission. An impulsive rocket burn is applied opposite to the orbital velocity at R_0. At the perihelion of the elliptic orbit, the sail is deployed impulsively, radially, and giving the sailcraft a lightness number equal to 1. This generates an escape rectilinear trajectory with a cruise speed equal to twice the parabolic speed at R_0

The analysis performed above is as simple as striking: specific values have been reported, but the result about the cruise speed depends only on the initial circular orbit. Two observations:

1. To achieve a final high speed, the spacecraft first has to lose most of its initial kinetic energy, about 65.7 %, independently of the initial orbit. Subsequently and closer to the Sun, the radiation pressure will be able to give the sailcraft much higher energy.
2. If one wants to achieve 84 km/s of excess speed (cruise speed) by a single rocket (tangential) impulse at 1 AU (where $V_{\text{circ}} = 29.785$ km/s), from the energy equation, it is straightforward to carry out $\Delta V = 64.2$ km/s, a huge impulse, a "mission impossible" for rockets.

Much probably, the above mission concept will be unfeasible for a number of reasons that are beyond the scopes of this book; nevertheless, it is meaningful from a theoretical viewpoint. As a point of fact, we will consider again such scenario later (see Fast and Very Fast Sailing), when we discuss realistic high-speed sailcraft trajectories.

INTERPLANETARY TRANSFERS

General Keplerian orbits are based on sailing always orthogonal to the local sunlight direction as sensed in SOF. The general control of a sail is expressed via the lightness vector in the vector Eq. (20.1). We discussed the **L**-vector and the sailcraft acceleration components in Chap. 19. Here, we summarize the dynamical role of the lightness components in order to introduce the reader to the interplanetary transfers. Then, we will show a number of meaningful examples of them.

Apart from the solar-wind and the gravitational perturbations from solar system bodies, a heliocentric sailcraft undergoes three fields when the sail is arbitrarily oriented in SOF: (1) the Sun's local gravity, (2) the *radial* sunlight-pressure force component, and (3) the *orthogonal* sunlight-pressure force component. Fields 1 and 2 are conservative; in contrast, field 3 is non-conservative. It is a strange behavior due to field splitting. From Chap. 19, we highlight:

1. The orbital energy, though depending on l_x, can be increased/ decreased if $l_y \neq 0$, or $\mathrm{d}l_x/\mathrm{d}t \neq 0$, or both.
2. The angular momentum can be changed in direction only if $l_z \neq 0$.
3. The angular momentum can be varied in magnitude only via $l_y \neq 0$.

The utilization of these properties allows the mission analyst to design any interplanetary transfer flight. Of course, a mathematical algorithm of optimization, with equality and inequality constraints, produces a set of locally optimal trajectories. The problem of which is the best one for a certain mission depends on the characteristics of the whole project one is dealing with. (This is the most difficult astrodynamical problem to be solved for each planned mission.)

Most interplanetary solar-sail transfers have been envisaged of rendezvous type. Although such rendezvous transfers are from the heliocentric orbit viewpoint only (i.e., the gravitational fields of the departure and arrival planets have not been considered), they are of significant historical meaning. The departure and the arrival may be approximately viewed as position-velocity states on the so-called spheres of gravitational influence. Furthermore, to illustrate the main trajectories properties, some flights have been supposed to be coplanar with the planetary orbits (this is not true, of course, but this approximation allows one to focus on the principal properties of the transfer trajectory). Nevertheless, the authors have re-computed such profiles in the modern view expressed in Chap. 19. One of the most meaningful novelties is the introduction of variable thermo-optical parameters, such as those shown in Figs. 19.4 and 19.5. When appropriate, we will comment on such results.

Figure 20.3 shows the 1987–1988 Earth-to-Mercury rendezvous transfer. As is apparent, the sail has to be kept at a negative azimuth in SOF for slowly decreasing its distance R from the Sun. For over 3 months, the sailcraft speed V decreases slowly as well; then, although the sail attitude angle continues to be negative, V begins increasing because of the lower R. In the last month of the transfer, the sail azimuth is positive for progressively matching the orbital velocity of Mercury. The total transfer lasts 345 days. An interesting three-dimensional transfer from the real Earth orbit to the real Mercury orbit can be computed for the 2020–2021 opportunity. A combination of transfer time and perihelion of the transfer trajectory can be optimized to 382 days/0.33 AU, respectively, with only three simple attitude maneuvers in SOF.

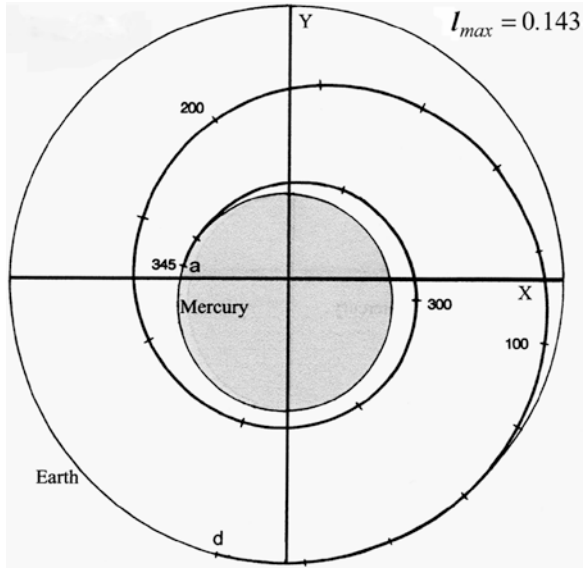

20.3 Example of Earth-to-Mercury transfer via solar sailing. Departure date was June 7, 1987. The maximum lightness number (but not achieved in the trajectory profile) is 0.143 (Adapted from [1], Courtesy of Taylor & Francis Group)

Apart from the attitude strategy, one should note that the sailcraft has to be transferred in orbital energy from –0.5 to –1.292, while its orbital angular momentum has to change from 1 to 0.609, in solar units. Such changes are enormous with respect to the current propulsion capabilities. Let us digress for a moment. An enlightening example comes from the next 2-spacecraft cornerstone mission by ESA and JAXA, named BepiColombo, for exploring Mercury deeply. BepiColombo should be set off in July 2016 on a journey to Mercury where it should arrive in January 2024! The transfer from Earth to Mercury is remarkably complicated. The spacecraft will be set on its interplanetary trajectory after a launch by Ariane. On its way to Mercury, the spacecraft shall employ a total of eight flybys at Earth, Venus, and Mercury!. BepiColombo will use solar-electric propulsion too.

When approaching Mercury, BepiColombo will use the planet's gravity and a conventional rocket engine to insert itself into the target polar orbit. Like many other important NASA and ESA missions, the astrodynamical realization of the flight depends completely on the relative positions of some planets; in other words, the launch window is very narrow, its repeatability is very low, and the transfer time is long. The authors have checked that, if sailcraft technology with a lightness number of 0.16 had been ready in 2013 (it was not), then the real heliocentric transfer to Mercury would have last 367 days. Mission opportunities would repeat more than one in every year and in different months, since there is no flyby need for gaining delta-V. Earth escape could be performed by a launcher providing a small hyperbolic excess speed, whereas Mercury capture (via solar sailing) may be aided by a small-size chemical engine. To within a quarter of a century (or less), Earth–Mercury–Earth regular round-trips may become a reality for many scientific missions via solar-photon sailing, if the major space agencies do not close their minds.

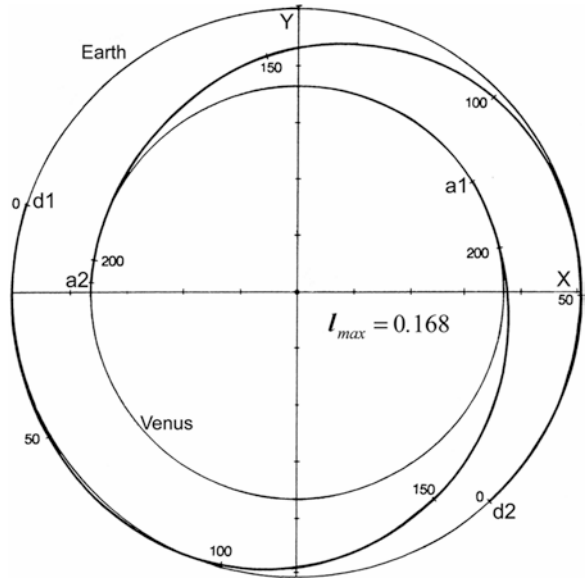

20.4 Two examples of Earth-to-Venus transfer via solar sailing with maximum lightness number equal to 0.168. Departures were on August 5, 1981 and March 4, 1983 (Adapted from [1], Courtesy of Taylor & Francis Group)

Figure 20.4 shows two Earth-to-Venus rendezvous transfers, in 1981–1983, lasting about 204 and 213 days, respectively. Sailcraft technology has been assumed to perform $l_{\max} = 0.168$, or 1 mm/s^2 as characteristic acceleration. In each profile, most of the trajectory is a decelerating arc, and then the final orbit matching occurs via a slight accelerating arc. For the future, we have computed a good 218-day opportunity with departure on December 6, 2019 (using the same technology). As opposed to missions to Mercury, good launches repeat every 20 months; transfer times can be different among them essentially because of the Venus orbit inclination (about 3.4°) over the ecliptic, and Earth and Venus orbit nodes (which differ by about 100°, on the average).

Figure 20.5 shows an example of Earth-to-Mars rendezvous transfers in 2033, as computed by author Vulpetti. (Earth and Mars orbits are those corresponding to 2033–2034). Let us at once say that there are many, many opportunities of rendezvous with Mars in the next two decades. We have chosen an overall "medium-technology" sailcraft with a total sail loading of 10 g/m^2 and a 425-day journey to Mars. This σ-value is about one order of magnitude better than the ESA Geosail mission concept. The small squares in Fig. 20.5 mark the departure, the arrival, and two intermediate attitude maneuvers. Thus, the minimum-time attitude control is piecewise-constant in HOF, and is simple to implement. One can suppose that even using a moderate sailcraft technology as a whole, a rather large sail could be designed realistically in the 2030s. Thus, if a 1-km^2 sail could be managed, a 10-tonne (1 tonne = 1 metric ton) ferry sailcraft would go forth and back between Earth and Mars, most probably with a gross payload of 6 tonnes; in that period, many infrastructures on the Mars surface would be presumably built. NASA, JAXA,

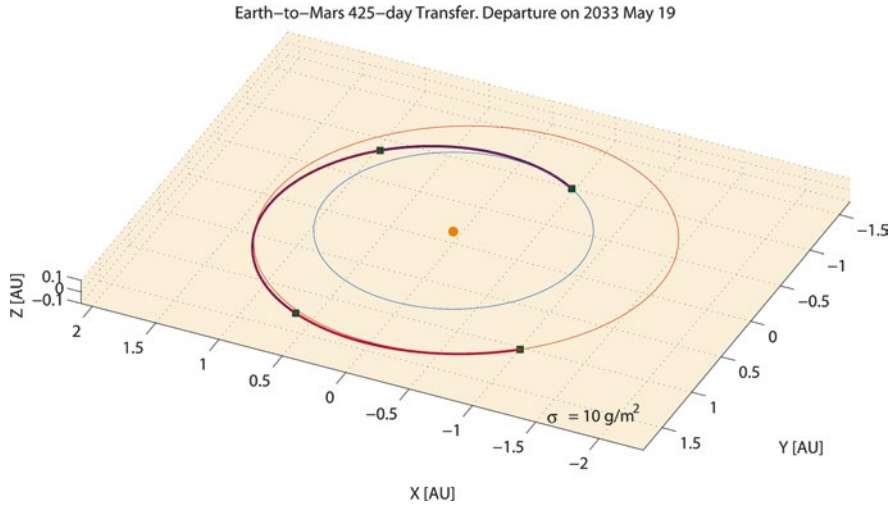

20.5 A 10-g/m^2 sailcraft minimum-time trajectory to Mars. Departure is on May 19, 2033; arrival is on July 19, 2034. *Squares* denote departure, arrival, and intermediate attitude maneuvers. The three trajectory arcs correspond to three SOF-constant attitudes. Specular and diffuse reflection and absorption of light by the Aluminum reflective layer have been realistically considered in the thrust model for this trajectory profile. (author Vulpetti, 2008, courtesy of Springer)

China, and ESA may have their ferries for Mars colonization. Of course, the set of trajectories of ferry sailcraft is more complex than what we have shown here; some of the related concepts hold, though.

Sailcraft can go to the planets beyond Mars. However, we do not present trajectory profiles here because the celestial-mechanics concepts of inner and outer spheres of influence could not be neglected for the distant large planets of the solar system. Only a few examples can be found in the specialized literature, but they refer to sailcraft "entering" some unstated sphere of planetary influence with too high a speed for ignoring a number of problems. The design of even simple sailcraft trajectories to the outer planets is beyond the scope of this chapter.[1]

Now, we shall show three figures of significant historical importance; the trajectory that a large sailcraft—envisaged, studied, and fostered by the Jet Propulsion Laboratory (JPL)—would have followed to rendezvous with the Halley comet in 1986. However, NASA headquarters did not approve the mission, and the history of solar sailing changed. However, who knows? Perhaps, if that very complicated mission had failed for some unexpected reason, public opinion would have been that the mission was unimpressive,

---

[1] At the time of this writing, there are rumors that JAXA has been working on a sailcraft aimed to go to Jupiter; however, at least to the authors' knowledge, no technical paper has been published hitherto.

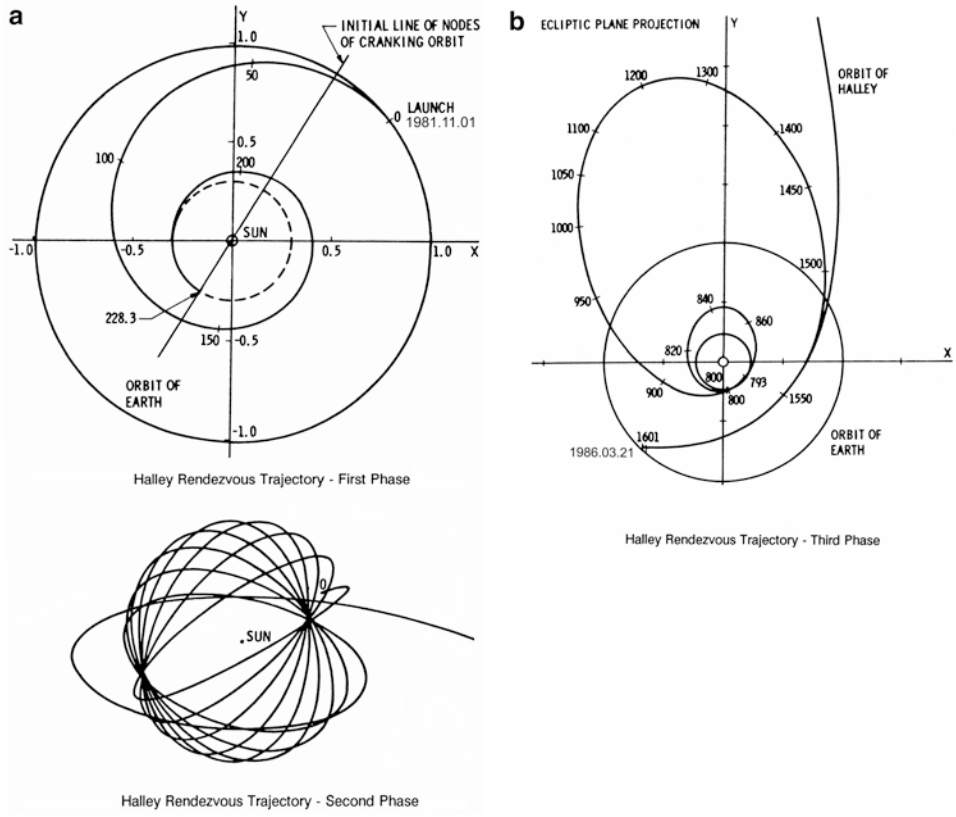

20.6 Halley comet rendezvous trajectory as designed by the Jet Propulsion Laboratory in 1970s. The conceived sail was a square of 800 m on each side; sailcraft sail loading was 7.7 g/m^2, and the maximum lightness number was equal to 0.177. (**a**) Two phases of the full transfer to Halley. (**b**) Retrograde trajectory arc to arrive at the comet post-perihelion rendezvous (Courtesy of NASA)

and now neither NASA nor other big space agency would be engaged in solar sailing, the authors of this book included!

Figure 20.6 shows the three phases of the full trajectory to Halley. JPL conceived a square sail with 800-m side, allowing a sailcraft sail loading of 7.7 g/m^2 and maximum lightness number equal to 0.177. After ballistic injection into the solar field (at 3.5 km/s) and sail deployment, the sailcraft is controlled such to spiral down and move to a circular orbit at 0.25 AU, but inclined 20° with respect to the ecliptic plane (see *ecliptic* in the Glossary). This completes the first transfer phase, as plotted in Fig. 20.6 (top left). In the second phase, shown in Fig. 20.6 (bottom left), the sailcraft maneuvers in attitude and changes the inclination of its osculating orbits until about 145° are achieved. As we know, orbits with inclination higher than 90° are retrograde. As a point of fact, not only is Halley comet strongly inclined with respect to the ecliptic, but also its motion is opposite to that of the planets, namely, it is clockwise. The sailcraft cranking in this phase can be described as a circular orbit slowly rotating about an axis lying on the ecliptic (i.e., the axis indicated

at the top of the figure). The third phase consists of a slow increase of energy and angular momentum parallel to that of the comet, as shown in Fig. 20.6 (right), due to the relatively low lightness number. The sailcraft approaches the comet from below, resulting in a post-perihelion rendezvous (a bit less than 1 AU). Then, the sail system is jettisoned so the spacecraft moves with the comet and eventually lands on it.

Some comments are in order: *First*, a similar mission accomplished by some electric engines would be hugely expensive. *Second*, the first two phases of the above trajectory design suggest a way to send a sailcraft over the solar poles, namely, in an orbit literally orthogonal to the solar equator. Some concepts of sailing to the solar poles are based on such a trajectory strategy. *Third*, a rendezvous near the comet's perihelion (~0.58 AU) would be desirable for scientific purposes. *Fourth*, at the time of the above JPL rendezvous mission concept, the *H*-reversal theory (which could be appropriate also for rendezvous with other retrograde-motion comets) was not yet set up. Even if it had been, 7.7 g/m^2 would have been too high for getting sailcraft motion reversal. *Fifth*, both solutions to the general equations to solar-photon sailing may be utilized for fast intercepting near Earth asteroids, e.g. see [2–4]. *Sixth*, according to JPL, the next Halley's perihelion will occur on May 31, 2061. There is plenty of time for designing a sailcraft using new technologies. Together with the progress already made in solar-sailing Astrodynamics, all that will certainly result in a completely new, much faster, and adjustable rendezvous trajectory, and robots for exploring and probing the comet.

These topics may be developed or analyzed still further in original Ph.D. dissertations mainly for graduate students in Astrodynamics or Aerospace engineering.

NON-KEPLERIAN ORBITS

When one talks about Keplerian orbits, either conventional or generalized (see General Keplerian Orbits, above), one implicitly assumes a basic fact: the instantaneous plane of the orbit passes though the barycenter of the central body. This holds even in many-body dynamics via the concept of osculating orbit. Now, let us suppose that all components of the lightness vector are nonzero except l_y (the transversal number). According to Eq. (19.9), the sailcraft thrust acceleration in HIF has no azimuthal component. In addition, according to points 1 and 3 on page 229, the sailcraft's angular-momentum magnitude and orbital energy are constant. In contrast, the angular momentum changes in direction; this excludes any set of circular orbits, the planes of which contain the solar center of mass. Do such factors have a more direct geometrical meaning? Yes, they have. A particular, but rich, family of orbits has been investigated in detail. However, by theoretical and numerical tools, it is possible to show that there exists a special class of non-Keplerian orbits described by:

$$\mathbf{R}(t) = \mathbf{s} + \mathbf{C}(t), \quad \mathbf{s} \cdot \mathbf{C}(t) = 0 \tag{20.3}$$

where $\mathbf{s}$ is a constant vector and $\mathbf{C}(t)$ is the vector position of either a circular or elliptic orbit perpendicular to $\mathbf{s}$. In other words, we can get circles or ellipses on planes not passing through the Sun! Vector $\mathbf{s}$ is just the shift of the orbital plane. In the past years, shifted circular orbits have been well studied from many interesting viewpoints, including

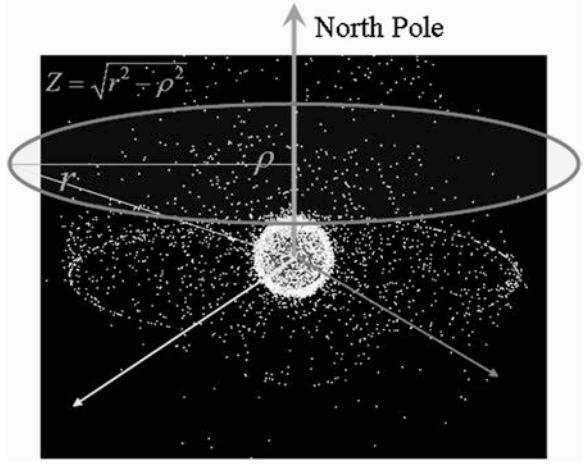

20.7 Displaced geostationary orbit for telecommunications over Earth's North Pole (Courtesy of NASA; adapted by author Vulpetti)

potential applications. In contrast, the larger family of shifted ellipses have been studied limitedly, probably because of its higher mathematical complexity. We have checked numerically that ellipses orthogonal to arbitrary shift vectors surely exist in the case of *ideal* sails. Of course, their geometrical properties are tightly related to the lightness vector and, as a consequence, to the sail technology and the evolution of the sail materials in the space environment (see Chap. 21).

The above feature holds also for planetocentric sailcraft, in particular Earth-bound. Applications of shifted circular and elliptic orbits maybe various. At the end of the 1980s, Robert L. Forward suggested utilizing some displaced geostationary orbit (GEO) for allowing telecommunications over Earth's poles, which cannot be seen by conventional GEO satellites just for the reason that their planes have to pass through the Earth's center of mass. He made preliminary calculations and invited colleagues to pursue further studies. In 2005, author Vulpetti, for his lectures at the Aerospace School of Rome University, computed aluminized-sail operational orbits and showed the relationships between orbit displacement, orbit period, pole elevation angle, and sailcraft sail loading. A simple example of shifted GEO orbit is shown in Fig. 20.7. This operational orbit is outside the zone of danger due to space debris (in the figure, the white dots represent a sort of visual mean distribution of space debris according to NASA). Table 20.1 contains the main parameters related to such an orbit.

The reported numbers are self-explanatory. The ultra-low value of the sail loading entails a factor of 800 in technological improvement with respect to the ESA Geosail mission concept. It should not be possible to increase appreciably the distance of the sailcraft from Earth so that the local gravitational acceleration is significantly lower. As a point of fact, even polar-zone telecommunications imply (1) reasonable elevation angles (the sailcraft is seen from any observer on ground), and (2) the requirement that voice-telecom should not have a time delay higher than the current 0.25 s. The users of GEO telecom satellites have all experienced annoyance from this delay during telephone conversations

Table 20.1. Main parameters relatively to the nominal shifted geostationary orbit, shown in Fig. 20.7 for observing terrestrial zones around the North Pole.

Operational-orbit period	86164.0989 s (1 sidereal day)
Sailcraft elevation at North Pole	11 degrees
Orbit displacement (Z)	2.211 Earth radii
Orbit radius (ρ)	6.2300 Earth radii
Sail distance (*r*)	6.6107 Earth radii
Lightness number (λ) {Sun, Earth}	{12.65, 0.334}
Sailcraft sail loading (σ)	0.1215 g/m^2

especially on the job. The analysis of realistic-sail-shifted ellipses (or quasi-ellipses) should be another topic of frontier Astrodynamics, to be addressed in M.S. theses or Ph.D. dissertations.

Recently, new families of non-Keplerian orbits have been discovered by Heiligers and McInnes [5]. Though the calculations were made by assuming an ideal sail, particular families should arise when the sailcraft motion is restricted to cylindrical or spherical surfaces through appropriate attitude control laws, which are function of the sailcraft's orbital acceleration. Sets of quasi-periodic or true-periodic orbits have been found. If such properties were confirmed for a *realistic*-physics sail, then amazing applications of solar-system science would be possible (depending on the sail-system technology of course). Incidentally, once again, none of the related envisaged missions would be accomplishable by rocket-craft.

MANY-BODY ORBITS

The many-body problem in celestial mechanics is known not to have a general analytical solution except for the two-body and the restricted three-body problems. Nevertheless, the many-body system is well managed numerically, as shown in several successful space missions. The JPL ephemeris file DE-430 is an excellent example of that. However, even the restricted two-body solar sailing (Sun plus sailcraft), as drawn from Eq. (20.1) with $\boldsymbol{P}=0$, exhibits no general closed-form solution, even in the two-dimensional case. There exist special solutions, though, in the restricted Sun–planet–sailcraft problem, namely, two primaries plus an infinitesimal mass body sensitive to the pressure of the light emitted by either primary. These particular solutions can be found if one assumes that:

1. the primaries (of masses M_1 and M_2) revolve on circular (coplanar) orbits about their common barycenter,
2. the sail has *specular* reflectance (which may be lower than 1, but with no diffuse component), and
3. the sail attitude is fixed in the baricentric reference frame (BRF), which is the frame co-rotating with the primaries.

In problems of this kind, what matters is to find the sailcraft's position and velocity histories in BRF.

The mathematical analysis of such a problem proceeds similarly to the well-known restricted three-body problem, with primaries moving in circles. The classical problem exhibits five equilibrium points (of which three are unstable) in the circles plane. However, in the current case, one has three more parameters: the sail loading σ or, equivalently, the lightness number (if the sail is perfectly reflecting), and the two angles specifying the sail orientation $\mathbf{n}$. In principle, σ and $\mathbf{n}$ can be chosen arbitrarily. Given a set $\{\sigma, \mathbf{n}\}$, the sailcraft has a certain *radial* number and, as discussed above (see General Keplerian Orbits), sees the luminous primary with reduced mass $M_1^* = (1 - l_x)\, M_1$ (here, l_x is assumed to be less than 1). As a result, there are equilibrium points for the equivalent restricted problem with primaries $\{M^*_1, M_2\}$; if there is a nonzero *normal* number, then such points are expected to be displaced with respect to the common plane of the primaries' motion. Varying the parameters $\{\sigma, \mathbf{n}\}$ in a continuous range entails an infinite set of equilibrium points, which are quite *local* and *relative* in nature, namely, they are sensed only by the sailcraft. (One might call them *artificial* equilibrium points, but one should remember that different sailcraft sense different equilibria, in general). In this context, there are *allowed* three-dimensional space regions of equilibrium points *induced* by the full set of values $\{M_1, M_2, \sigma, \mathbf{n}\}$. If $\sigma \to \infty$ (i.e., a spacecraft without sail), then one finds the classical Lagrange points again.

What about a sailcraft that moves in the Earth–Moon system? By using the mathematical tool known as the theory of perturbations, it is possible to investigate many features dependent also on the particular mass ratio $M_{\text{Moon}}/M_{\text{Earth}} = 0.0123$ of such system. For example, *above* the classical Lagrange points, sailcraft may move on an elliptic displaced orbit, but active control is required; in other words, sail attitude has to be trimmed to compensate for secular effects.

What about a sailcraft that is placed in the Sun-Earth system ($M_{\text{Sun}}/M_{\text{Earth}} = 333{,}000$)? Perturbative analysis of sailcraft dynamics shows that the equilibrium points are generally unstable. However, due to the very small perturbation accelerations around them, a sail orientation trimming strategy should be sufficient for getting a long stay of the sailcraft around these points.

Some of the above considerations even hold for a rocket-powered spacecraft. For instance, NASA spacecraft ACE (Advanced Composition Explorer) has been orbiting around the classical L_1 point of the Sun–Earth system. This libration-point orbit is unstable and four to six station-keeping maneuvers per year are required to keep the spacecraft bound to L_1. The overall fuel consumption per year amounts to about 4.1 kg (9 lb). There is sufficient fuel onboard to allow operations until 2022. However, ACE (or similar spacecraft) would be unable to find long-term equilibrium in arbitrary regions of the Sun–Earth gravitational system. Although they are conceptually possible, the fuel to be spent via any control strategy would be enormous or expensive at least. This is not the case for sailcraft, as we already know.

Colin McInnes (now at University of Strathclyde, Glasgow, UK) has studied for years halo orbits and their potential applications. They have many problems that are not yet investigated due to the huge complexity of the many-body problem. For instance, suitable research on special realistic-sail-induced equilibrium regions under the influence of the

Sun and a number ($N>2$) of planets would be high desirable. Again, this could be the subject of Ph.D. dissertations. Potential applications, not known so far, may arise.

On a completely different scale, recently, a team of Italian researchers at Pisa University [6] analyzed the behavior of an ideal balloon under the influence of two stars, namely, a restricted three-body problem with radiation pressure due to two stars, e.g. those ones in the Alpha Centauri A/B system. This work began extending the cases of previous papers [7, 8], and is part of the MIRA Collaboration. This collaboration is an Italian inter-university no-profit scientific work about physical, mathematical, and technological aspects regarding special future sailcraft carried by a starship to a nearby star, hopefully launched within the twenty-first-century towards the stellar system of Alpha Centauri. A starship of this type is currently under theoretical investigation in the Project Icarus. At the time of this writing, University of Rome *La Sapienza* and University of Pisa have been participating in MIRA, which is coordinated by author Vulpetti.

FAST AND VERY FAST SAILING

Let us resume the CRS reference mission described earlier. We can distinguish two semi-open intervals of speed[2]: (1) $\left[V^{circ}, V^{parab}\right)_{R_0}$, and (2) $\left[V^{parab}, V^{star}\right)_{R_0}$. If a sailcraft endowed with a certain sail loading can be guided such a way that its *cruise* speed belongs to interval-1, then the sailcraft is said to perform a *fast* solar sailing. If the cruise speed falls in open interval-2, then we talk about *very fast* solar sailing. Thus, the CRS reference flight represents a "conceptual attainment" of the (otherwise arbitrary) lower bound of the very fast range. Below, we discuss the upper bound V^{star}.

The theory of fast and very fast solar sailing is a rather complex topic of solar sailing Astrodynamics. It was formulated only in the mid-1990s [9, 10], and only recently, it has been deeply investigated [11–15]. This intriguing research is beyond the scope of this book. Nevertheless, we will explain the basic principles qualitatively and, as done in the previous sections of this chapter, show some examples from our computer programs, which are able to consider a large number of effects known hitherto for getting a realistic trajectory of high-speed sailcraft.

Although the original description of high-speed sailcraft trajectories was different from what we are discussing, it is useful to begin with an earlier observation. For simplicity, let us consider a two-dimensional flight: a sailcraft starts its sail-powered flight from a circular orbit about the Sun. Suppose that the maximum lightness number is in the open interval (1/2, 1). If there were only the radial number non-vanishing, then we know from our earlier discussion that the sailcraft trajectory would be hyperbolic, but with decreasing speed. Let us take a specific, but meaningful example: $l_x = 0.725$. This sailcraft, starting from Earth's orbit, would have a speed of almost 20.1 km/s at 100 AU from the Sun (a speed higher than the Voyager-1 cruise speed). Now, let us think of a different sail control strategy for the *same* sailcraft: the sail is tilted such that $l_x = 0.534$ and $l_y = -0.242$ (this is possible for a realistic aluminized sail with $\sigma = 2$ g/m^2, $\alpha = -25.9°$ and a surface mean roughness

---

[2] With respect to the 1st edition of this book, these intervals have been changed a bit in order to reflect the new studies about escaping from the solar system.

of 10 nm, according to Eqs. (19.3a)–(19.3b), and Figs. 19.4 and 19.5). What happens? Because the radial number is higher than ½, the sailcraft first moves outward from the initial circular orbit (as above), but now both angular momentum and energy progressively decrease because the transversal number is negative and sufficiently high. Geometrically, the first effect entails that the angle between the sailcraft's position and velocity vectors increases gradually, whereas the second effect implies that speed decreases more quickly than in a pure hyperbolic orbit.

Eventually, a point P^* in space *may* be reached at time t^*, where vector position and velocity, both different from zero, are anti-parallel, namely, the orbital angular momentum $\mathbf{H}$ vanishes; in addition, in P^* the orbital energy achieves its absolute minimum in the flight. Why "*may*"? Because there are two special options: (1) immediately before P^*—in principle, in the infinitesimal interval (t*-dt, t*)—the sailcraft is commanded to carry out an impulsive attitude maneuver for obtaining the sail's opposite azimuth, +25.9°; or (2) the sail azimuth is kept at –25.9°. The first case entails an obvious acceleration while the motion continues to be direct (or counterclockwise); in other words, $\mathbf{H}=0$ is not achieved. A seemingly strange situation happens for the second case: the sailcraft accelerates as well! Why? After reaching $\mathbf{H}=0$, $\mathbf{H}$ reverses, namely the angle from the position vector to the velocity vector becomes progressively greater than 180°, and the motion becomes clockwise. As a result, a negative azimuth in retrograde motion means acceleration, does it not? Thus, in both cases, the sailcraft accelerates toward the Sun and can actually fly by the star along different paths. However, our surprises are not finished. It can be shown mathematically that the perihelion in each case is *not* the point of maximum speed (as in either classical or generalized Keplerian orbits). Past the perihelion (at 0.20 AU), the sailcraft continues to accelerate until a maximum speed value (83.8 km/s) is achieved very soon. Subsequently, the speed decreases (but not so much) with another striking feature. Due to the radial number that balances more than a half of the solar gravity (at any distance) and to the transversal number that does not cease accelerating the vehicle, the sailcraft speed exhibits a sort of plateau past the initial circular departure orbit. Differently from parabolic and hyperbolic orbits, one can speak of cruise phase indeed.

The attentive reader could argue, OK, it is a fine and intriguing behavior of (nonlinear) solar sailing; but will we gain anything? Well, we above reported a speed of 20 km/s at 100 AU for an intuitive sailcraft control. Now, accurate calculations show that practically the cruise speed amounts to 70 km/s for any $R>9$ AU. We stress that the sailcraft is the same; only the attitude control strategy is different and is constant in SOF again! As a result, this sailcraft is able to reach 100 AU after 7.9 years from launch, instead of 23.2 years. Figure 20.8 shows this case of motion reversal. In particular, the sail orientation in HIF is shown (remember that it is constant in SOF). The capital letters in the figure label special points in chronological order: M maximum distance from the Sun; P, minimum speed; Q, $\mathbf{H}=0$; S, energy vanishes, namely, the escape condition is met; U, perihelion, and W, maximum speed.

The example discussed above is only one element of the large mission class of fast sailing. Figure 20.9a shows how the trajectory profile changes with the negative transversal number and the radial number higher than ½ Note than the motion reversal happens even for lightness numbers lower than that considered above. Figure 20.9b shows the corresponding hodographs. Of course, the unit circles denote the Earth velocity evolution (here

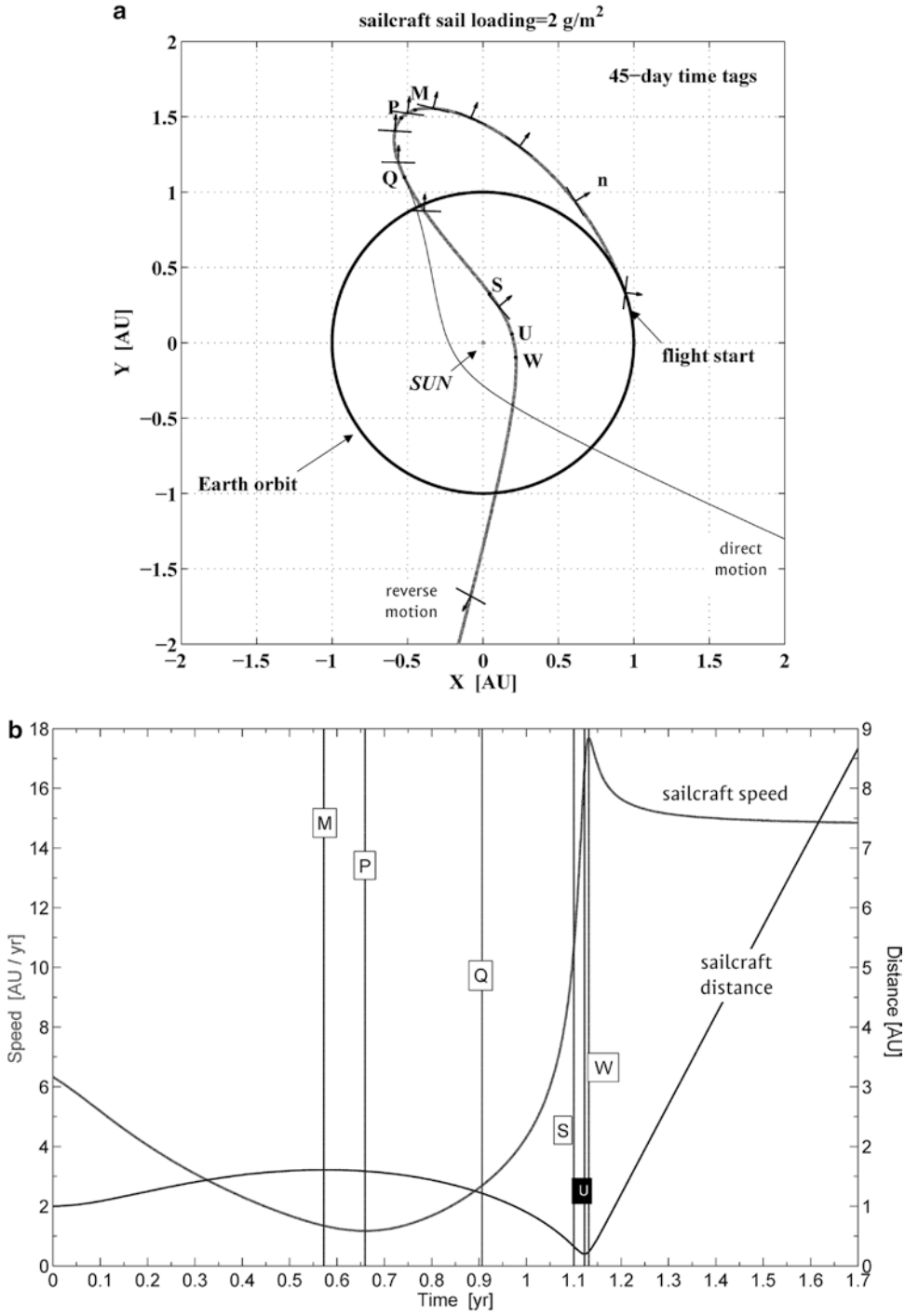

20.8 Example of *fast solar sailing*. Sun flyby via 2D motion-reversal for escaping the solar system; sailcraft technology is of 2 g/m^2. (**a**) Pre-perihelion and post-perihelion trajectory arcs with constant-in-SOF sail attitude. The second profile (*thinner line*), starting from point Q, shows the symmetric direct-motion trajectory. (**b**) Time behaviors of the Sun–sailcraft distance and sailcraft speed. The time tags are described in the text

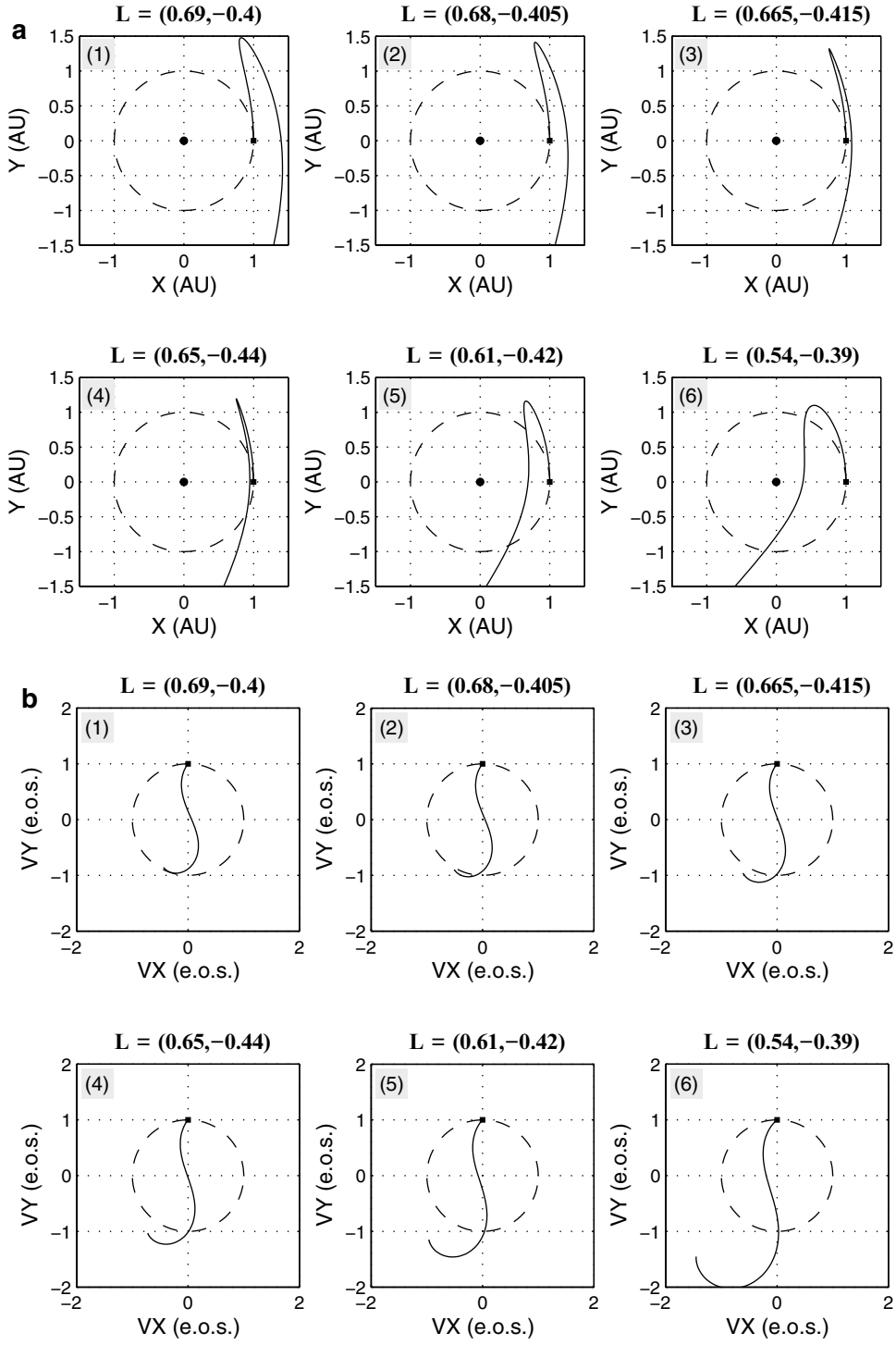

20.9 (**a**) Angular-momentum reversal as a function of the negative transversal number and the radial number higher than 1/2; (**b**) Hodographs of the trajectories plotted in (**a**). The unit circle denotes the Earth velocity evolution (here assumed to be circular for simplicity). Velocity unit is the earth orbital speed (e.o.s.), or 2π AU/year

assumed as circular for simplicity). Plots are self-explanatory. In particular, note how each hodograph evolves by reversing the curvature vector. The final speeds in the last two examples are considerably higher than the speed of the departure planet.

Note 2: We have emphasized sailing mode 2. Trajectory of sailing mode-1 is different in the second part, namely, from point Q on. However, both cruise speed and transfer time are exactly equal to those ones of mode 2. This is due to the symmetry of such sailing modes. If you draw the line passing through the Sun (at the origin O) and the point Q, then either trajectory arc can be gotten from the other one by a 180° rotation about this line. Then, the final path directions are different. However, this is a very good thing. As a point of fact, by shifting the launch date by some months (depending on the lightness number), one finds *two* launch opportunities per year, *every year*, for rapidly escaping from the solar system toward a prefixed direction. Said differently, the dependence on the relative positions of planets to give energy to spacecraft (often through many flybys) will be only a vague memory when light and large solar sails are made and managed in space.

Note 3: The perihelion value is rather sensitive to the sail attitude. Small midcourse attitude maneuvers may be accomplished to satisfy trajectory constraints. After perihelion, some large attitude maneuver could be designed and safely performed to optimize some index of performance, for example, the time to target.

The 2D trajectories discussed hitherto are ideal; no real sailcraft can strictly move in a plane for a number of reasons. At first glance, this may seem plain; in fact, there are attitude errors, planetary and environmental perturbations, and unmodeled forces. However, there is a non-intuitive cause. If the third component of the lightness vector, which we named the normal number (l_z) in Chap. 19, is different from zero in any finite time interval wherein one requires $\mathbf{H} = 0$, then the trajectory *torsion* diverges as the angle (φ) from **R** to **V** approaches 180°, no matter how small l_z may be. That brings about a new sailcraft trajectory class (which is three-dimensional and is driven by a sail attitude profile that is not as easy as that above) exhibiting motion reversal. The analysis of such a class involves not only energy and angular momentum, but also trajectory torsion. It can be proved that the $|\mathbf{H}|$ does not vanish, but passes through a minimum much lower than the angular momentum of the sailcraft departure orbit. After the time of such minimum, the third component of **H** reverses and retains its new sign in receding from the Sun.

We would like to end this chapter by discussing an example of 3D motion-reversal very fast trajectory. The related mission was first presented and discussed at STAIF-2000 (Albuquerque, New Mexico) by author Vulpetti. Sail-system and spacecraft technology has been supposed such that $\sigma = 1.2$ g/m^2, namely, over three orders of magnitude better than IKAROS. The *maximum* lightness number is 1.21 (equivalent to a characteristic acceleration of 7.18 mm/s^2); that is, the sailcraft could, when necessary, thrust higher than the local gravitational acceleration. The nominal target of this extrasolar mission is {550 AU, ecliptic longitude = 86.8°, ecliptic latitude = 5.5°}. The distance value means the minimum distance of the Sun's gravitational lens (see Glossary) for photons (nothing dealing with gravitational waves); the direction is that from the Galaxy's center to the Sun (the galactic anti-center direction). Figures 20.10 summarize what may be of concern here. The trajectory arc around the Sun clearly shows that the sailcraft goes above the ecliptic by decelerating, and then sailcraft crosses the ecliptic after motion reversal. Perihelion

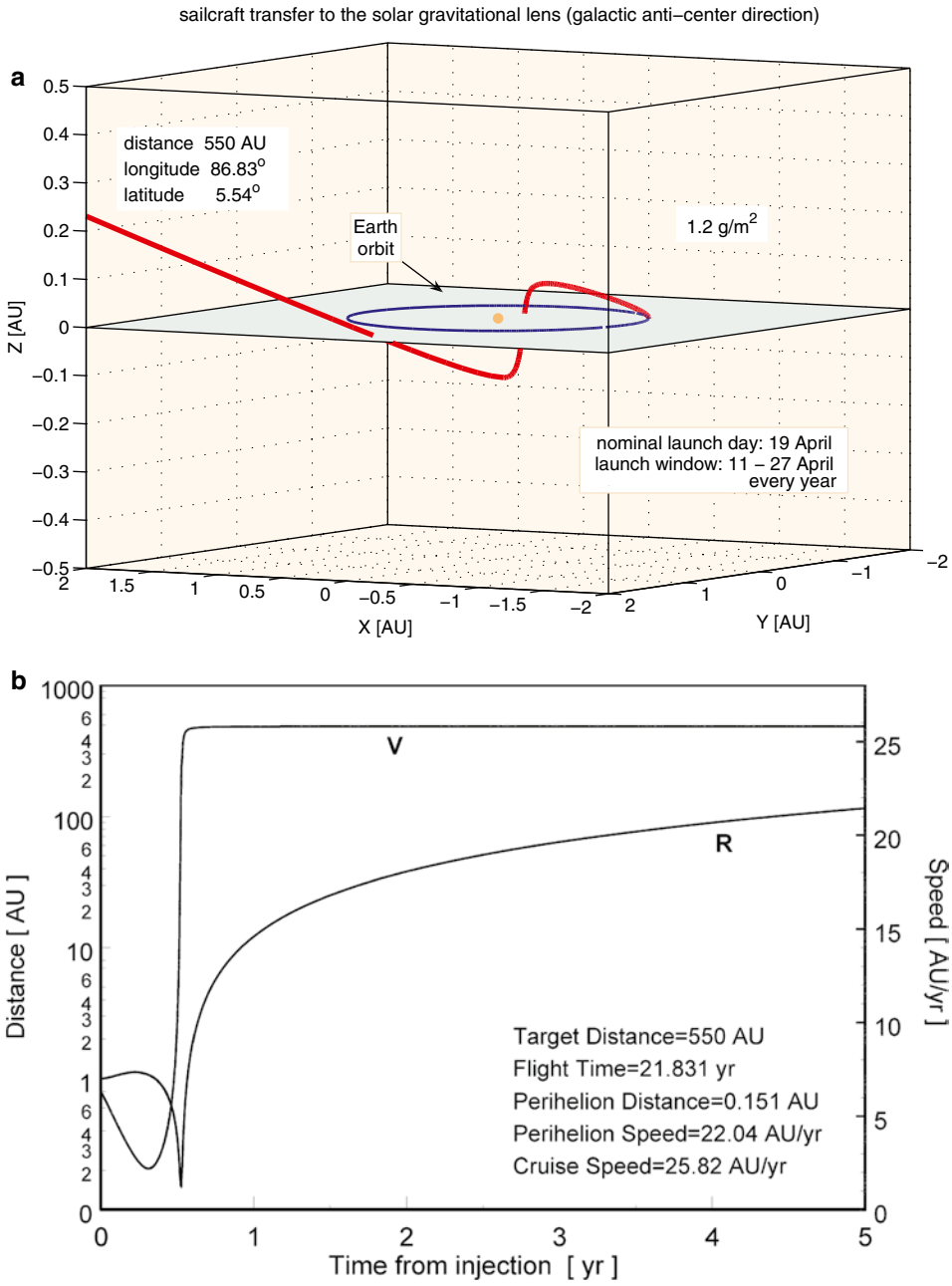

20.10 Example of 3D *very fast* solar sailing. Sailcraft escapes the solar system via motion-reversal and aims at the target distance of 550 AU. Sailcraft technology has been assumed to be *1.2* g/m^2. (**a**) Pre-perihelion and post-perihelion trajectory arcs, (**b**) Time behaviors of the Sun-sailcraft distance and sailcraft speed (Solar Sails, 1st edition, courtesy of Springer)

(0.15 AU) is below the ecliptic. The sailcraft reemerges still accelerating because now the optimal sail attitude entails a lightness number of 1.18. The time evolution of sailcraft speed and distance are plotted in Fig. 20.10b. The effect of having a sailcraft sail loading sufficiently below the critical density is manifest in the speed behavior: no local maximum takes place. Strictly speaking, if the sail is not jettisoned at few astronomical units, the sailcraft continues to accelerate because the sum of the accelerations is $+0.18\ \mu_\odot/R^2$ outward. If one jettisons the sail at, for example, 5 AU, the speed loss is 8 % of the cruise speed. Since a high-technology sail may also work as a multifunction object, there is no compelling reason for jettisoning it inside the solar system; this may be accomplished beyond the heliopause. Note the square-root-like shape of $V(t)$ with a cruise value of 25.82 AU/year, or 122.4 km/s, or almost three times the escape speed from the solar system at Earth's orbit. According to the criteria set at the beginning of this section, this is a very fast solar-sail mission. The 550-AU target distance is achieved in less than 22 years.[3] A 16-day launch window is found in April, *every year.*

Numerical experiments, regarding Sun flybys via either motion-reversal or motion-direct, have shown that this highly nonlinear effect in solar sailing is possible only if the sailcraft sail loading is lower than 2.10-2.20 g/m^2, depending on how the thrust model is accurate. If medium-term technology exhibits higher values, then *two* direct-motion solar flybys may be used to increase the cruise speed for escaping the solar system. However, one does not get the same cruise speed of the single flyby! The difference between these two modes is significant and depends on the actual σ-value.

Finally, what about the above-mentioned upper bound V^{star}*?* The superscript *star* means that it depends also on the star that emits light. Is appears obvious that some limit (somewhat less than c) should exist from a couple of evident facts: (1) the Sun has a finite temperature and radius, and (2) the sailcraft sail loading cannot be made arbitrarily small. We suggest some considerations related to dynamics, nanotechnology and space environment (see Chap. 21). As a result, the following very simple expression, $V^{star} = 2\pi\sqrt{2l_{max} / R_{min}}\ \left[\mathrm{AU / year}\right]$, is a good reference value for the maximum (realistically attained)speed by future advanced sailcraft. Note that, if high lightness number is achieved after the separation of a spacecraft from the (remaining) sailcraft having another spacecraft as payload, then $l_{\max}$ pertains to this sailcraft.

Projected nanotechnology (from current research) might allow $l \simeq 30$, e.g. for tiny sailcraft discussed by author Matloff [16], while the minimum reachable distance (by such sailcraft) from the Sun might be $R_{min} = 0.05$ AU. Then, $V^{star} \simeq 218$ AU/year $\simeq 1030$ km/s $= 0.0034\,c$. The future of solar-photon sailing, in the context of the so-called interstellar precursor missions [17], appears exciting enough.

---

[3] At the time of this writing, Voyager-1 is far 126.8 AU from the Sun and is running off with a speed of 3.5 AU/year (http://voyager.jpl.nasa.gov/). Independently of the antenna working, this Voyager will reach 550 AU in the autumn of 2134. If the above (or like) sailcraft were launched in 2027 (i.e. 50 years *after* the Voyagers), it would achieve 550 AU in 2049, i.e. 85 years *before* Voyager-1! A nanotech-based fast sailcraft is not required to flyby many planets to get much energy for escaping from the solar system. One Sun flyby is necessary and sufficient for tapping much more energy.

FURTHER READING

http://adsabs.harvard.edu/abs/1979Sci…205.1133E.
http://archive.ncsa.uiuc.edu/Cyberia/NumRel/EinsteinTest.html.

REFERENCES

1. 1.J. L. Wright, *Space Sailing*, Gordon and Breach Science Publishers, 1992
2. *15.*G. L. Matloff, The Solar Collector and Near-Earth Object Deflection, Vol. 62, No. 4–5, February–March 2008, pp. 334–337
3. 16.G. L. Matloff, Deflecting Asteroids, IEEE Spectrum, March 28, 2012
4. 10.X. Zeng, H. Baoyin, J. Li, and S. Gong, Earth-crossing asteroids deflection with a sailcraft, 3rd International Symposium on Solar Sailing, June 11-13, Glasgow, 2013
5. 14.J. Heiligers and C. McInnes, New Families of non-Keplerian Orbits: Solar Sail Motion over Cylinders and Spheres, 3rd International Symposium on Solar Sailing, June 11-13, Glasgow, 2013
6. 13.G. Aliasi, G. Mengali, and A. A. Quarta, Artificial Equilibrium Points for a Solar Balloon in the Alpha Centauri System, 8th IAA Symposium on the Future of Space Exploration: Towards the Stars, Turin, July 3-5, 2013
7. 11.J. F. L. Simmons, A. J. C. McDonald, and J. C. Brown, The Restricted 3-Body Problem with Radiation Pressure, Celestial Mechanics, **35** (1985), 145-187
8. 12.V. V. Markellos, E. Perdios, K. Papadakis, The stability of inner collinear equilibrium points in the photo-gravitational elliptic restricted problem, Astrophysics and Space Science, Vol. 199, No. 1, 1993, pp. 139-146
9. 2.G. Vulpetti, *Missions to the Heliopause and Beyond by Staged Propulsion Spacecraft*, 43rd IAF Congress, paper IAA-92-0240, at The World Space Congress, Washington D.C., 1992(published by the American Institute of Aeronautics and Astronautics, New York).
10. *4.*G. Vulpetti, *Sailcraft at High Speed by Orbital Angular Momentum Reversal, Acta Astronautica 1997, 40: 733–758*
11. *3.G. Vulpetti,3D high-speed escape heliocentric trajectories by all-metallic-sail low-mass sailcraft,* Acta Astronautica 1996; 39: 161–170
12. G. Vulpetti, Sailcraft-Based Mission to The Solar Gravitational Lens, STAIF-2000, Albuquerque (New Mexico, USA), 30 Jan - 3 Feb, 2000
13. *7.*G. Vulpetti, *Fundamentals and Progress of Solar-Photon Sailing*, Lectures at Dept. of Astronautical Engineering of Rome University 'La Sapienza', April-May 2013, in /SolarSailing/SailPhotonPhysics of http://www.giovannivulpetti.it
14. *6.G. L. Matloff, G. Vulpetti, C. Bangs, R. Haggerty, The Interstellar Probe (ISP): Pre-Perihelion Trajectories and Application of Holography, NASA/CR-2002-211730, June 2002.*
15. 8.G. Vulpetti, Fast Solar Sailing: Astrodynamics of Special Sailcraft Trajectories, Springer, 2012
16. 5.G. L. Matloff, Deep-Space Probes, 2nd ed., Springer-Praxis, Chichester, UK, 2005.
17. *17.*Studies by the International Academy of Astronautics, Key Technologies to Enable Near-Term Interstellar Scientific Precursor Missions, May 2013